JPP Journal of Pharmacy and Pharmacology

JPP 2004, 56: 1109–1118
© 2004 The Authors
Received April 26, 2004
Accepted June 15, 2004
DOI 10.1211/0022357044193
ISSN 0022-3573

Fluorescein permeability and electrical resistance of human skin during low frequency ultrasound application

Limary M. Cancel, John M. Tarbell and Abdellaziz Ben-Jebria

Abstract

Transdermal drug delivery offers an alternative to injections and oral medication but is limited by the low skin permeability of most drugs. The use of low-frequency ultrasound over long periods of time, typically over an hour, has been shown to enhance skin permeability, a phenomenon referred to as sonophoresis. In this study, we investigated the effects of short time sonication of human skin at 20 kHz and at variable intensities and duty cycles on the dynamics of fluorescein transport across the skin (permeability) as well as the changes in the skin's structural integrity (electrical resistance). We found that a short application of ultrasound enhanced the transport of fluorescein across human skin by a factor in the range of 2–9 for full thickness skin samples and by a factor in the range of 2–28 000 for heat-stripped stratum corneum samples (however, samples with very high (10^3) enhancement were likely to have been damaged by ultrasound). The electrical resistance of the skin decreased by an average of 20% for full thickness samples and 58% for stratum corneum samples. Increasing the duty cycle from 10 to 60% caused a significant increase in permeability enhancement from 2.3 to 9.1, and an increase in intensity from 8 to 23 mW cm^{-2} induced a significant increase in permeability enhancement from 2 to 7.4, indicating a clear dependence of the permeability on both duty cycle and intensity. The increase in solute flux upon ultrasound exposure was immediate, demonstrating for the first time the fast response dynamics of sonophoretic enhancement. In addition, a quantitative analysis of the thermal and convective dispersion effects associated with ultrasound application showed that each contributes significantly to the overall permeability enhancement observed.

Biomolecular Transport Dynamics Laboratory, Department of Chemical Engineering, The Pennsylvania State University, University Park, PA 16802, USA

Limary M. Cancel, John M. Tarbell, Abdellaziz Ben-Jebria

Correspondence: L. M. Cancel, Department of Biomedical Engineering, The City College of New York/CUNY, Steinman Hall, Convent Avenue at 140th St. New York, NY 10031, USA. E-mail: lcancel@student.ccny.cuny.edu

Acknowledgement and funding: We would like to thank Osama Al-Bataineh and Dr Nadine Smith at The Pennsylvania State University for their collaboration and use of their laboratory facilities for the calibration of our sonicator. We would also like to thank Mila Ristic for her help in setting up experiments. This research was supported in part by the Applied Research Lab at The Pennsylvania State University.

Introduction

Transdermal drug delivery offers several advantages over traditional delivery methods by avoiding drug loss due to liver metabolism, providing sustained release of therapeutics and offering better patient compliance (Bronaugh & Mibach 1989). However, very few drugs are able to penetrate the skin by passive diffusion at a rate sufficient to make drug delivery viable.

The application of ultrasound has been shown to increase the low skin permeability for various drugs (sonophoresis) (Mitragotri et al 1995a, b, 1996). The mechanisms and applications of sonophoresis have been reviewed in the literature (Joshi & Raje 2002; Mitragotri & Kost 2004). Cavitation, the growth and collapse of gas bubbles, is generally recognized to be the dominant mechanism of sonophoresis. Cavitation is thought to disorder the lipid bilayers in the outermost layer of the skin, the stratum corneum, creating mass transfer pathways and thus increasing the diffusion coefficient of solutes. However, cavitation alone cannot account for the total mass transfer enhancement observed. Several mechanisms seem to contribute to this transport phenomenon, among them, structural changes caused by cavitation (Levy et al 1989; Mitragotri et al 1995b, 1996), thermal effects (Levy et al 1989; Suslick 1989; Bommannan et al 1992; Mitragotri et al 1995b), mixing in the liquid phase (Levy et al 1989) and acoustic streaming through hair follicles and sweat ducts (Tachibana & Tachibana 1993). In addition, the results of recent studies point to a convective mechanism of enhancement (Mitragotri et al 2000; Ristic 2000), although no quantitative analysis has been proposed.

The electrical resistance of the skin is a good instantaneous indicator of the structural properties of the skin (Allenby et al 1961). Due to significant hindrance of the ionic transport through the lipid bilayers, the electrical resistance of the skin is very high and, in most previous studies, it has been used to verify that the structural integrity of skin samples is within the normal range. However, the continuous monitoring of skin electrical resistance during ultrasound application can provide insight into the mechanisms governing the enhancement of mass transfer through this biological barrier.

As most previous studies examined the long-term (several hours) effects of sonophoresis, the principal aim of this study was to investigate the short-term (few minutes) effects of low frequency (20 kHz) ultrasound on the permeability of fluorescein (MW 376, solubility in H_2O 25 g L^{-1}) across stratum corneum and full thickness human skin. Fluorescein is a small hydrophilic molecule with a passive permeability through skin similar to that of sucrose. The effect of duty cycle and intensity on the enhancement and the dynamics of the skin's response to ultrasound were also examined.

Materials and Methods

Materials

Fluorescein and phosphate-buffered saline (PBS) were obtained from Sigma Chemicals (St Louis, MO). Fresh (non cadaver) human skin (both sexes, abdomen) was obtained from local clinics. Full thickness skin samples were prepared by removing the thick (3–5 cm) layer of fat. The skin was then stored in a freezer at −20°C for later use. Samples were defrosted immediately before performing the experiments on full thickness skin. For experiments on stratum corneum, heat stripping of full thickness samples was performed. Briefly, the full thickness skin was immersed in de-ionized distilled water at 60°C for 2 min followed by removal of the stratum corneum. The stratum corneum was then stored at 4°C and 95% humidity for up to 2 weeks. The Institutional Review Board of The Penn State University Research Protections approved the use of anonymous human skin samples.

Ultrasound equipment

Low frequency ultrasound was applied with a sonicator operating at 20 KHz (Model XL2020; Misonix Inc., Farmingdale, NY), using a tapered microtip probe (diameter 1/8", microtip area 0.08 cm^2). The sonicator was operated in a pulsed mode with duty cycles of 10, 20, 40 and 60% and an intensity level of 8–24 mW cm^{-2}. In all cases the pulse repetition period was 1 s.

The free-field intensity of the ultrasound was measured using a hydrophone (Model TC4033; Reson Inc., Goleta, CA) placed 1 cm below the transducer tip in a large water tank. The compressional (P_c), rarefactional (P_r) and root-mean-square (P_{rms}) pressure amplitudes were recorded using an oscilloscope (Agilent 54622A, 100 MHz). The spatial peak–temporal peak (I_{sptp}) and spatial peak–temporal average (I_{spta}) intensities were calculated from the pressure amplitudes by:

$$I_{sptp} = \frac{P_{peak}^2}{\rho c} \qquad I_{spta} = \frac{P_{rms}^2}{\rho c} \tag{1}$$

where P_{peak} is the larger of P_c and P_r, ρ is the density of water (kg m^{-3}) and c is the speed of sound in water (m s^{-1}).

Measurement of fluorescein concentration

Fluorescein concentrations were measured using a dye fluorometer (C&L Instruments, Hummelstown, PA) by collecting samples (140 μL) periodically. The fluorescence of the samples was determined at characteristic fluorescein excitation and emission wavelengths of 485 nm and 535 nm, respectively.

Fluorescein transport

The transport experiments were conducted in a modified, custom made, Franz diffusion cell (A.B. Seal Glassblowing Spec. Inc., Bellefonte, PA) which consists of two glass compartments, the donor compartment having a volume of about 1 mL, and a receiver compartment having a volume of about 7 mL. These two compartments were clamped together after mounting the skin sample with the stratum corneum side facing the donor compartment. The cross-section exposed to ultrasound had a diameter of 0.9 cm. In the experiments using stratum corneum, a flat rubber ring was placed below the membrane to seal and to prevent the membrane from being scratched by the edges of the diffusion cell. Both compartments were filled with PBS, and the fluorescein was added to the donor compartment. At the beginning of each experiment the levels of fluid in the donor and receiver compartments were balanced and the system was equilibrated for at least 30 min to eliminate a hydrostatic pressure gradient across the skin. A magnetic stir bar provided mixing in the receiver compartment. All the experiments were carried out at room temperature (~293 K). The temperature of the solution immediately above the skin was measured periodically by inserting a standard thermocouple into the donor compartment.

The permeability (P_e) of the skin is given by:

$$P_e = \frac{J}{C_D - C_R} = \frac{V_R}{AC_D}\frac{dC_R}{dt} \tag{2}$$

where J is the flux of fluorescein, C_D and C_R are the concentrations in the donor and receiver compartments, V_R is the volume of the receiver compartment, A is the surface area of the skin, dC_R/dt was calculated from the measured concentration profiles in the receiver compartment by least-square regression and we have assumed that C_R is negligible compared to C_D. Separate regression lines were obtained for the passive, sonophoretic and recovery portions of the concentration profile. The permeability

enhancement was defined as the sonophoretic permeability divided by the passive permeability of the skin.

Passive permeability
The donor compartment was filled with a fluorescein solution (~530 μM) and the receiver compartment was filled with PBS. The concentration in the receiver compartment was monitored by withdrawing 140-μL samples every 30 min for a minimum of 2 h. The amount of solution removed from the receiver was immediately replaced with fresh PBS. The passive permeability across human skin was found to be $4.24 \times 10^{-9} \pm 1.73 \times 10^{-9}$ cm s^{-1} and $5.58 \times 10^{-9} \pm 2.33 \times 10^{-9}$ cm s^{-1} for full thickness skin and stratum corneum samples, respectively.

Sonophoretic permeability
Immediately following the measurement of passive permeability, the tip of the ultrasound transducer was introduced in the donor compartment and placed about 8 mm above the skin. Low frequency ultrasound was applied in a pulsed mode in the range 10–60% and at intensity levels in the range 8–24 mW cm^{-2}. The concentration in the receiver compartment was monitored by withdrawing 140-μL samples after 1.5, 6, 15 and 30 min of sonication. For the experiments where the duty cycle or intensity was varied, samples were withdrawn from the receiver 1.5, 6, 10 and 15 min after each step change of the operating conditions. In every case, the amount of solution removed from the receiver compartment was immediately replaced with fresh PBS. The concentration in the donor compartment was monitored by withdrawing 20-μL samples at the beginning and at the end of each experiment. The recovery of the permeability after sonication was monitored by measuring the concentration of fluorescein in the receiver compartment every hour for at least 4 h after the sonication was terminated.

Electrical resistance of the skin

Electrical resistance was measured by means of a pair of Ag/AgCl electrodes (InVivo Metrics, Heraldsburg, CA). An AC field, having a voltage of 100 mV and a frequency of 10 Hz, was applied for a short period of time (typically 15 s) using a function generator (Model 3011B; BK Precision, Chicago, IL). A resistor ($R = 54\,k\Omega$) was connected in series with the diffusion cell to allow determination of the small ($\sim 1 \times 10^{-6}\,\mu A$) current through the circuit by measuring the voltage drop across the known resistance. In addition, the added resistance stabilized voltage measurements across the diffusion cell and minimized unwanted reactions on the surface of the electrodes, thus ensuring accurate voltage measurements and increasing the electrode lifetime. The voltage drop across the diffusion cell (U_{cell}) and across the resistor (U_R) were measured using digital multimeters. Applying Ohm's law to the resistor and the diffusion cell leads to the following expression for the resistance of the diffusion cell (R_{cell}):

$$R_{cell} = R \cdot \frac{U_{cell}}{U_R} \qquad (3)$$

The PBS resistance was calculated separately using the same set-up without mounting the skin. Considering the PBS and the skin as two resistors connected in series, the resistance of the skin was found by subtracting the PBS resistance from the measured resistance of the diffusion cell. Samples having resistance below $10\,k\Omega \cdot cm^2$ were discarded. The resistance was monitored during ultrasound application by stopping the sonicator for a short period of time (typically 30 s) to make the measurement. Skin resistance was also monitored after ultrasound application, typically for a period of 4 h.

Statistical methods

The data for the electrical resistance and fluorescein permeability of the skin is presented as normalized values. The electrical resistance was normalized by the initial resistance and the permeability was normalized by the passive permeability of the sample. The values for electrical resistance and permeability presented are means ± s.e. Statistical significance was analysed by *t*-test or, when multiple treatments were employed, by analysis of variance. $P < 0.05$ was used as the significance level for the statistical analysis.

Results and Discussion

General effect of ultrasound on the permeability of stratum corneum and its electrical resistance

The electrical resistance and permeability to fluorescein of 11 stratum corneum samples was monitored during ultrasound application (20 kHz, 10% duty cycle, 8 mW cm^{-2}). The flux of fluorescein increased within 2 min of ultrasound application and was found to remain constant (at this increased value) for the entire period of sonication. Once the ultrasound was turned off, the solute flux immediately returned close to its original baseline value. Straight lines were used to fit the concentration profiles. A typical concentration profile is shown in Figure 1.

The behaviour of the electrical resistance and permeability was found to fall in one of two regimes. First, when the electrical resistance of the samples decreased by an average of 47%, a significant ($P < 0.04$) enhancement in permeability of 5.1 ± 1.8 times the baseline value was obtained (Table 1, Figure 2). Five minutes after sonication, although the electrical resistance increased only slightly from its value immediately after turning the ultrasound off, the permeability returned close to its original baseline value (0.7 ± 0.2 times its baseline value, $P > 0.05$). Second, when the electrical resistance decreased beyond 50% (up to an average of 75%, Figure 2), the permeability of the stratum corneum was variable, with an enhancement that ranged from 465 to 28 000 (data not shown). The recovery of permeability for the samples in this regime was also quite variable, fluctuating between 7 and 800 times the baseline value (data not shown). The recovery of electrical resistance after sonication in this regime was found to be minimal (Figure 2). One possible explanation for this wide range of permeability

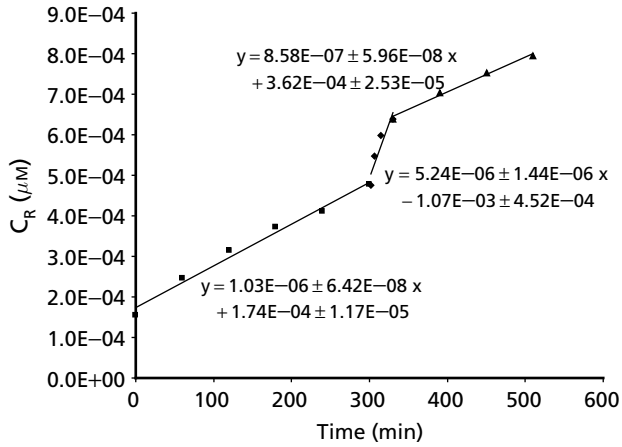

Figure 1 Typical concentration profile for a 30-min sonication experiment using stratum corneum. Squares show the passive flux of fluorescein (C_R = concn in receiver compartment), diamonds show the flux during the 30-min sonication and triangles show the flux after the ultrasound has been turned off.

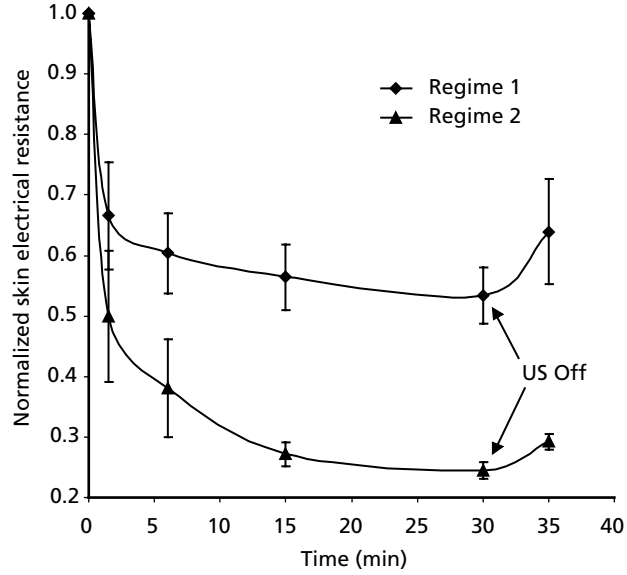

Figure 2 Variation of the normalized stratum corneum electrical resistance upon ultrasound exposure (10% duty cycle, 8 mW cm^{-2}), Regime 1 (diamonds) and Regime 2 (triangles). Ultrasound (US) exposure began at time = 0 and ended where indicated. Data are means ± s.e., n = 6 or 4 for Regime 1 and 2, respectively.

enhancement and large drop in resistance is an irreversible mechanical stretching or deformation of the tissue caused by oscillation and vibration of the tissue upon exposure to ultrasound. The extent of the deformation may depend on the elastic properties of the stratum corneum, which can vary from sample to sample. These stratum corneum samples were probably damaged by the ultrasound and therefore these results are not typical. It was observed that large, irreversible, permeability enhancements were obtained only for samples for which the drop in electrical resistance was larger than 70%. Our results indicate that this may be the threshold value between the two regimes.

Figure 2 shows that the drop in electrical resistance is immediate and largest during the first 2 min of sonication and then slowly approaches a plateau after the initial large drop. For the samples in Regime 1, after an initial drop of 33% in the first 2 min of ultrasound exposure, the electrical resistance dropped by only 14% during the remaining 28 min of sonication. Similarly, for the samples in Regime 2, an initial electrical resistance drop of 50% in

Table 1 Summary of permeability results for all experimental conditions

Protocol	Tissue type	Duty cycle	Intensity	Normalized permeability
30 min sonication	Stratum corneum			
During US		10%	8 mW cm^{-2}	5.1 ± 1.8*
Post-US		—	—	0.7 ± 0.2
30 min sonication	Full thickness			
During US		10%	8 mW cm^{-2}	5.2 ± 1.2*
Post-US		—	—	0.9 ± 0.2
Variable duty cycle	Full thickness			
Step 1		10%	8 mW cm^{-2}	2.3 ± 0.3*
Step 2		40%	8 mW cm^{-2}	4.4 ± 0.7**
Step 3		60%	8 mW cm^{-2}	9.1 ± 2.6**
Post-US		—	—	1.9 ± 0.5
Variable intensity	Full thickness			
Step 1		10%	8 mW cm^{-2}	2.0 ± 0.3*
Step 2		10%	15.4 mW cm^{-2}	4.0 ± 0.9
Step 3		10%	23.4 mW cm^{-2}	7.4 ± 2.0**
Post-US		—	—	0.8 ± 0.2

US, ultrasound. *$P < 0.05$ vs baseline; **$P < 0.05$ vs Step 1.

the first 2 min was followed by a drop of only 25% in the remaining time of sonication. Since the drop in electrical resistance is believed to be due to the disordering of the lipid bilayers by cavitation bubbles, these results suggest that cavitation effects occur rapidly, but reach a plateau beyond which no more pathways can be opened despite continued ultrasound application. This may be due in part to decreased availability of cavitation nuclei in the liquid medium (Mitragotri et al 1995b).

Both permeability and resistance were monitored for a long period of time (4 h) after sonication. The permeability of the stratum corneum was found to be constant during this period of time while its electrical resistance did not deviate significantly from the value obtained 5 min after sonication. In the case of the samples in Regime 1, the permeability returned close to its original baseline value, while the electrical resistance recovered partially (by an average of 11%). These results indicate that (passive) diffusion through the disordered lipid bilayers can not account completely for the observed permeability enhancement. It is clear that, in addition to opening diffusion pathways by cavitation, ultrasound provides an additional driving force for mass transfer that further enhances the permeability of the stratum corneum. In Regime 2, while the permeability returned to a value higher than the original baseline of passive diffusion, there was virtually no recovery of electrical resistance. For these samples, it appears that the structural changes caused by cavitation were sufficient to enhance even the passive diffusion through the membrane. However, the enhancement observed for these samples was even larger when the ultrasound was on, indicating the action of an additional mechanism of transport, perhaps convective, which in conjunction with cavitation produces the total enhancement observed.

General effect of ultrasound on the permeability of full thickness skin and its electrical resistance

To evaluate the role of the supporting epidermis layer in the sonophoretic enhancement, full thickness skin samples were exposed to ultrasound (20 kHz, 10% duty cycle, 8 mW cm^{-2}) for 30 min. The electrical resistance of the skin decreased by a maximum of 16% (Figure 3). As with the stratum corneum, the largest drop in resistance was observed during the first 2 min of sonication. However, the skin began to recover its electrical resistance during sonication. Unlike the stratum corneum, the full thickness resistance increased significantly beyond its original baseline value ($P < 0.002$) immediately after turning off ultrasound. The average permeability enhancement was found to be 5.2 ± 1.2 ($P < 0.02$). After turning the ultrasound off, the permeability immediately decreased to 0.93 ± 0.17 times the baseline value (not significantly different from baseline, $P > 0.3$). These results are similar to those obtained for stratum corneum samples in Regime 1, with the main difference being the full recovery of the skin's electrical resistance after stopping the ultrasound. During these experiments we observed that the oscillation and vibration of the skin upon ultrasound application was greatly reduced.

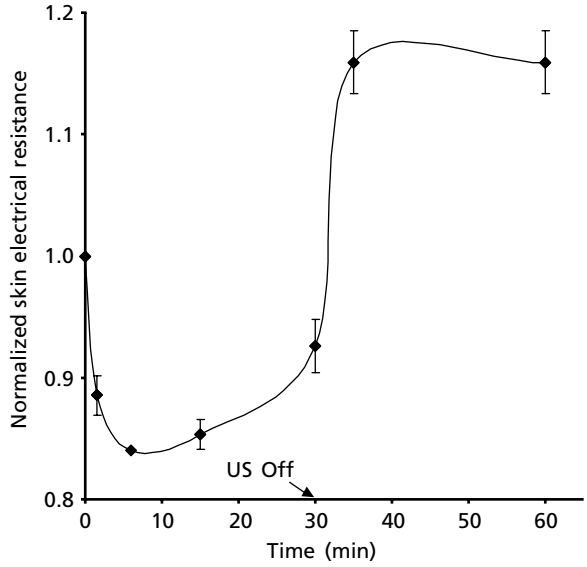

Figure 3 Variation of the normalized electrical resistance of full thickness skin samples upon ultrasound application (10% duty cycle, 8 mW cm^{-2}). Ultrasound (US) exposure began at time = 0 and ended where indicated. Data are means ± s.e., n = 5.

These findings suggest that the full thickness of the skin provides support to the stratum corneum and prevents irreversible mechanical stretching and deformation.

Effect of duty cycle on skin permeability and electrical resistance

To evaluate the effect of duty cycle on the measured skin parameters, a sample of full thickness skin was exposed to step changes of duty cycle from 10% to 40% to 60% while the intensity was kept constant at 8 mW cm^{-2}. At each of these step changes of duty cycle, the skin was sonicated for 15 min. The flux of fluorescein at each duty cycle was found to be nearly constant and straight lines were used to fit the concentration profiles, yielding a single value of permeability for each duty cycle.

Application of ultrasound to the full thickness skin induced a quick reduction in the electric resistance that reached a minimum of 86% of its baseline value during the 10% duty cycle phase (Figure 4A). A fast drop in skin resistance was subsequently observed in response to every step increase of duty cycle. After turning off the ultrasound, the skin electrical resistance recovered beyond its baseline value, reaching a maximum of 140% (significantly different from baseline, $P < 0.05$). Low frequency sonication of full thickness skin also induced an enhancement in permeability that was dependent on duty cycle. Fluorescein flux increased within 2 min after the duty cycle was elevated, indicating a fast response of the skin permeability to ultrasound. After reaching a maximum enhancement at 60% duty cycle (9.1 ± 2.6), the permeability decreased to 1.9 ± 0.5 times its original value, immediately after removal of ultrasound.

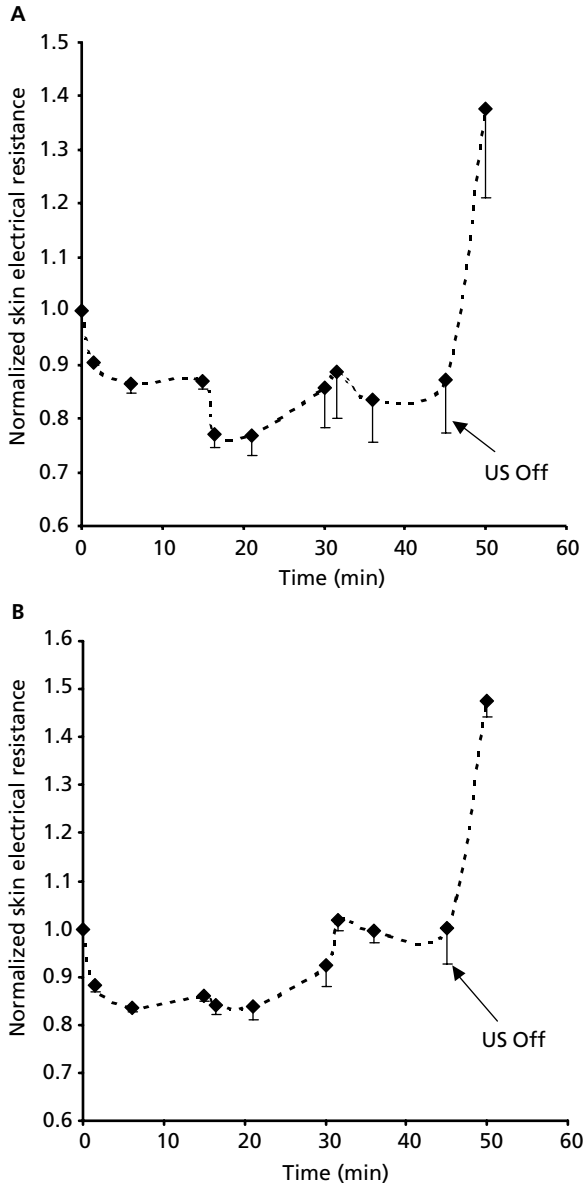

Figure 4 A. Effect of duty cycle on the variation of the normalized skin resistance during ultrasound (US) application (8 mW cm^{-2}, variable duty cycle) to full thickness skin. Data are means ± s.e., n = 5. B. Effect of acoustic intensity on the variation of the normalized skin resistance during ultrasound (US) application (10% duty cycle, variable intensity) to full thickness skin. Data are means ± s.e., n = 5.

These results for variable duty cycle confirm that other mechanisms acting in conjunction with cavitation are responsible for the observed permeability enhancement since the effects of cavitation on the structural integrity of the skin, as measured by the electrical resistance, were diminishing while the permeability continued to increase. In addition, the fast response of the skin's permeability (both enhancement and recovery) to sonication suggests a convective mechanism governing this enhancement. Our findings are consistent with those reported by Mitragotri & Kost (2000), who observed that the pressure wave provided an additional driving force for mass transfer, resulting in a larger enhancement when the ultrasound was left on than when the skin was only pre-treated with ultrasound. However, thermal effects and acoustic streaming through hair follicles and sweat glands, in addition to convection, might have contributed to the overall enhancement observed.

Effect of intensity on skin permeability and electrical resistance

To evaluate the effect of acoustic intensity on permeability and electrical resistance of full thickness skin, experiments were performed in a manner similar to that described above for duty cycle. In this case, the duty cycle was maintained at 10% and the intensity was increased every 15 min from 8 to 15.4 to 23.4 mW cm^{-2}. The initial 15 min of ultrasound application induced a fast reduction of 16% in the electrical resistance from its baseline value (Figure 4B). This reduction was not exceeded at any operating intensity for as long as ultrasound was applied. The skin resistance recovered significantly beyond its original value (147% of the baseline value, $P < 0.001$) once the ultrasound was terminated. Ultrasound caused an increase in permeability that was dependent on the acoustic intensity and reached a maximum of 7.4 ± 2 at 23.4 mW cm^{-2}. The return of permeability to its original passive diffusion level was complete after turning off the sonicator (0.80 ± 0.21).

Mechanisms

Among the mechanisms governing ultrasound-induced enhancement of the mass transfer of molecules through skin, cavitation, temperature elevation, acoustic streaming and convective dispersion are believed to be factors that may substantially contribute to the efficacy of low frequency ultrasound. Cavitation effects are generally recognized to be the dominant mechanism of sonophoretic enhancement. These effects are directly related to the observed drop in the electrical resistance of the skin. A porous pathway model relating skin resistance and permeability has been proposed (Tezel et al 2003). Using simple engineering models, quantitative analyses of the contributions of the remaining mechanisms (temperature, acoustic streaming and convective dispersion) are suggested in the following sections.

Effect of temperature

Table 2 shows that the application of ultrasound increased the temperature of the fluid in the compartment above the skin for all the experiments performed. It can be observed that the increase in temperature was in all cases higher for full thickness tissues than for the stratum corneum. These results suggest that the full thickness of the skin absorbs more acoustic energy than the stratum corneum. Most previous studies have used only the stratum corneum and reported an increase in temperature of ~7°C (Mitragotri et al 1995b). In-vivo, temperature effects are likely to be higher, similar to those encountered in-vitro with full thickness samples.

Table 2 Effect of temperature increase on the permeability enhancement across human skin as estimated by equations 4 and 5

Ultrasound parameters	10% Duty cycle ($8\,mW\,cm^{-2}$)	10% Duty cycle ($8\,mW\,cm^{-2}$)	Variable duty cycle ($8\,mW\,cm^{-2}$)	10% Duty cycle (variable intensity)
Tissue type	Stratum corneum	Full thickness	Full thickness	Full thickness
Max. temp. increase observed (°C)	5.74	7.92	26.52	15.24
Viscosity of water (cp)	0.885	0.848	0.584	0.722
Enhancement observed	5.1	5.2	9.1	7.4
Enhancement (due to temperature increase)	1.15	1.22	1.87	1.46
Enhancement % (due to temperature increase)	23	24	21	20

The increase in temperature increases the diffusion coefficient of fluorescein, thus increasing the permeability according to:

$$P_e = \frac{D_{eff} \cdot K}{L} \tag{4}$$

where P_e is the permeability ($cm\,s^{-1}$), D_{eff} is the effective diffusion coefficient ($cm^2\,s^{-1}$), K is the partition coefficient between the liquid phase and the membrane and L is the membrane thickness (cm). The effective diffusion coefficient can be represented as $D_{eff} = D\,H$, where D is the free diffusion coefficient and H is a function of the structure of the tissue.

Since the solutions used in this study were dilute, the Wilke–Chang equation (Bird et al 1960) can be used to estimate the dependence of the free diffusion coefficient (D) on temperature. This theory shows that

$$D\alpha\frac{T}{\eta} \tag{5}$$

where T is the temperature and η is the viscosity of the solvent (PBS). Assuming the viscosity of PBS is equal to that of water, and that neither K nor H (equation 4) are affected by temperature, the increase in permeability resulting from the maximum temperature increase observed in each experiment has been estimated in Table 2. Thermal effects can explain about 20% of the overall enhancement. While this is only a portion of the total enhancement, it is clear that thermal effects play a role in sonophoresis.

Effect of acoustic streaming

Exposure to ultrasound can generate fluid velocities in a porous medium, a phenomenon termed acoustic streaming. Fluid velocities can enhance transport by inducing convective mixing of the solute. In the skin, this process occurs mainly in the sweat glands and hair follicles (Edwards & Langer 1994). When the skin is exposed to low frequency ultrasound, convective transport through the aqueous pores of the corneocytes made available by cavitation can also occur.

The convective velocity generated by ultrasound in a cylindrical pore scales as (Gooberman 1968):

$$U \approx \frac{R_p^2 I\alpha}{\mu c} \tag{6}$$

where R_p is the radius of the pore, I is the intensity of the ultrasound, α is the absorption coefficient of the fluid, μ is the fluid viscosity and c is the sound velocity in the medium. The radii of sweat ducts, hair follicles and corneocytes pores has been estimated by Edwards & Langer (1994) to be 5 μm, 1 μm (annular space of follicle) and 1.8 nm, respectively. With these estimates, equation 8 yields convective velocities of $2.3 \times 10^{-8}\,cm\,s^{-1}$ (sweat ducts), $9.2 \times 10^{-10}\,cm\,s^{-1}$ (hair follicles) and $2.7 \times 10^{-15}\,cm\,s^{-1}$ (corneocytes pores). While the convective velocities generated through sweat ducts and hair follicles are comparable to the permeability of fluorescein through the skin, the area fraction of each of these routes is small enough (7.9×10^{-5} for sweat ducts and 1.9×10^{-4} for hair follicles (Edwards & Langer 1994)) to make the convective flow through them negligible.

Effect of convective dispersion

Time-periodic convection may give rise to significant dispersion, even when the net convection is zero (Brenner & Edwards 1993). Convective dispersion phenomena in pores arise from the non-uniformity of the solute velocity across the pore cross section. Taylor (1953) showed that the dispersion process, for times sufficiently long to allow radial molecular diffusion across the velocity field, obeys a convective-dispersion equation and the axial Taylor dispersivity ($\overline{D}^*$) may be expressed as the sum

$$\overline{D}^* = \overline{D}^M + \overline{D}^C \tag{7}$$

of a hindered axial molecular diffusion coefficient $\overline{D}^M$ and a convective dispersion coefficient $\overline{D}^C$. The calculation of these two coefficients is presented in the Appendix. Table 3 shows the contribution of the convective dispersion to the total dispersivity. Also shown are the criteria established by equations A10 and A11. Note that in these calculations R_P refers to the radius of an aqueous pore through a corneocyte. That is, we have assumed that the transcorneocyte route of transport has been made available by the effects of cavitation. It can be seen from Table 3 that a small, but still present, enhancement in the total dispersivity is provided by convective dispersion.

Summary and conclusions

In the past, sonophoresis studies have primarily evaluated the effect of long-term ultrasound application, typically

Table 3 Contribution of convective dispersion through corneocytes to the permeability enhancement

I ($W\,cm^{-2}$)	$\overline{V}$ ($cm\,s^{-1}$)	L/R_P	N_{Pe}	Re	$\overline{D}^C$ ($cm^2\,s^{-1}$)	$\overline{D}^*$ ($cm^2\,s^{-1}$)	$\overline{D}^*/\overline{D}^M$
0.008	0.73	8333	6.23	0.0000131	1.38×10^{-9}	2.25×10^{-8}	1.07
0.015	1.00	8333	8.53	0.0000180	2.58×10^{-9}	2.37×10^{-8}	1.12
0.023	1.24	8333	10.56	0.0000223	3.96×10^{-9}	2.51×10^{-8}	1.19

$\overline{D}^C$, convective dispersion coeffiecient; $\overline{D}^M$, hindered axial molecular diffusion coefficient; $\overline{D}^*$, the total axial dispersivity (equation 7). The ratio $\overline{D}^*/\overline{D}^M$ represents the enhancement in dispersivity provided by convective dispersion. Values used for the calculations were: $a = 0.485$ nm (determined using Lydersen's method (Lydersen 1955) with group contributions to critical volume obtained from Polling et al (2001)); $L = 15\,\mu m$; $\rho = 1000\,kg\,m^{-3}$; $R_P = 1.8$ nm (Edwards & Langer 1994); $\mu = 10^{-3}$ Pa s; $D_0 = 6 \times 10^{-8}\,cm^2\,s^{-1}$; $H_C = 0.35$ (equation A1); $H_D = 0.23$ (equation A7).

from 1 to 5 h. Only recently, Mitragotri & Kost (2000) and Tang et al (2002) have shown the effectiveness of short exposure times on mannitol and inulin transport. Regardless of the ultrasound exposure time, all of the previous studies have neglected the short-term dynamics of the skin's response to ultrasound exposure. In this study, we have shown the rapid increase in solute flux upon ultrasound exposure by measuring the fluorescein concentration at intervals generally no longer than 5 min. In addition we have also shown a rapid decrease in solute flux immediately after the ultrasound is turned off. In this manner we have demonstrated the fast dynamic response of sonophoretic enhancement of skin permeability.

Most previous studies have used stratum corneum as a model system for in-vitro studies. While it is clear that the principal barrier to solute transport across the skin is the stratum corneum, the experiments performed in this study have demonstrated that the full thickness of the skin provides support and prevents irreversible damage caused by oscillations of the skin membrane upon ultrasound exposure. We have also demonstrated that the use of stratum corneum as an experimental model resulted in an overestimation of the ultrasound-induced enhancement of permeability, because of the probable alteration of its structural integrity.

Our experimental data suggest that the enhancement of fluorescein transport occurs through several mechanisms. During the first few minutes of sonication, cavitation presumably disorders the lipid bilayers, lowering the electrical resistance of the skin and opening pathways through which solutes can diffuse. However, we have shown that while the effects of cavitation quickly reach a plateau and the skin starts to recover its structural integrity (electrical resistance), the permeability enhancement is sustained.

Our data indicate that thermal effects can account for a portion (generally about 20%) of the mass transfer enhancement. The fast dose–response dynamic behaviour of the skin's response to ultrasound suggests a convective contribution to the enhancement induced by the ultrasound pressure wave. Acoustic streaming effects through hair follicles, sweat glands and the aqueous pores of the corneocytes were found to be negligible. The convective dispersion model, on the other hand, predicts an enhancement of 7–19%, depending on the intensity of the ultrasound. This corresponds to 16–20% of the enhancement observed. Note, however, that the convective dispersion process could take place only after the lipid bilayers have been disordered by cavitation, making transport through aqueous pores of the corneocytes possible. Therefore, we conclude that while the disordering of the lipid bilayers by cavitation is probably the dominant mechanism of sonophoresis, thermal effects and convective dispersion contribute significantly to the observed enhancement.

References

Allenby, A. F. J., Schock, C., Tees, T. F. S. (1961) The effect of heat and organic solvents on the electrical impedance and permeability of excised human skin. *Br. J. Dermatol.* **81**: 31–62

Bird, R. B., Stewart, W. E., Lightfoot, E. N. (1960) *Transport phenomena*. Wiley, New York, pp 514–515

Bommannan, D., Menon, G. K., Okuyama, H., Elias, P. M., Guy, R. (1992) Sonophoresis. II. Examination of the mechanism(s) of ultrasound-enhanced transdermal drug delivery. *Pharm. Res.* **9**: 1043–1047

Brenner, H., Edwards, D. A. (1993) *Macrotransport processes*. Butterworth-Heinemann Ser. in Chem. Eng., Stoneham, MA, pp 31–62, 132–139

Bronaugh, R. L., Mibach, H. I. (1989) In: *Percutaneous absorption: mechanisms, methodology, drug delivery*. Marcel Dekker, New York, pp 1–12

Edwards, D. A., Langer, R. (1994) A linear theory of transdermal transport phenomena. *J. Pharm. Sci.* **83**: 1315–1334

Gooberman, G. L. (1968) *Ultrasonics, theory and application*. English Univ. Press, London

Joshi, A., Raje, J. (2002) Sonicated transdermal drug transport. *J. Control. Release* **83**: 13–22

Leighton, T. G. (1994) *The acoustic bubble*. Academic Press, San Diego, CA, pp 1–65

Levy, D., Kost, J., Meshulam, Y., Langer, R. (1989) Effect of ultrasound on transdermal drug delivery to rats and guinea-pigs. *J. Clin. Invest.* **83**: 2074–2078

Lydersen, A. L. (1955) *Estimation of critical properties of organic compounds*. Univ. Wisconsin, Coll. Eng. Exp. Stn. Rep. No. 3, Madison, WI, April

Mavrovouniotis, G. M., Brenner, H. (1988) Hindered sedimentation, diffusion, and dispersion coefficients for Brownian spheres in circular cylindrical pores. *J. Colloid Interface Sci* **124**: 269–283

Mitragotri, S., Kost, J. (2000) Low-frequency sonophoresis: a noninvasive method of drug delivery and diagnostics. *Biotechnol. Prog.* **16**: 488–492

Mitragotri, S, Kost, J. (2004) Low-frequency sonophoresis: a review. *Adv. Drug Deliv. Rev.* **56**: 589–601

Mitragotri, S., Blankschtein, D., Langer, R. (1995a) Ultrasound-mediated transdermal protein delivery. *Science* **269**: 850–853

Mitragotri, S., Edwards, D. A., Blankschtein, D., Langer, R. (1995b) A mechanistic study of ultrasonically-enhanced transdermal drug delivery. *J. Pharm. Sci.* **84**: 697–705

Mitragotri, S., Blankschtein, D., Langer, R. (1996) Transdermal drug delivery using low-frequency sonophoresis. *Pharm. Res.* **13**: 411–420

Mitragotri, S., Farrell, J., Tang, H., Terahara, T., Kost, J., Langer, R. (2000) Determination of threshold energy dose for ultrasound-induced transdermal drug transport. *J. Control. Release* **63**: 41–52

Polling, B. E., Prausnitz, J. M., O'Connell, J. P. (2001) *The properties of gases and liquids*. 5th Edn, McGraw-Hill, New York, pp C2–C4

Ristic, C. (2000) *Ultrasonic enhancement of mass transfer rates across membranes*. PhD Thesis, Pennsylvania State University

Slutsky, A. S., Drazen, J. M., Ingram, R. H., Kamm, R. D., Shapiro, A. H., Fredberg, J. J., Loring, S. H., Lehr, J. (1980) Effective pulmonary ventilation with small-volume oscillations at high frequency. *Science* **209**: 609–611

Suslick, K. S. (1989) *Ultrasound: its chemical, physical and biological effects*. VCH Publishers, New York, pp 287–301

Tachibana, K., Tachibana, S. (1993) Use of ultrasound to enhance the local-anesthetic effect of topically applied aqueous lidocane. *Anesthesiology* **78**: 1091–1096

Tang, H., Blankschtein, D., Langer, R. (2002) Effects of low-frequency ultrasound on the transdermal permeation of mannitol: comparative studies with in vivo and in vitro skin. *J. Pharm. Sci.* **91**: 1776–1794

Taylor, G. I. (1953) Dispersion of soluble matter in solvent flowing slowly through a tube. *Proc. R. Soc.* **A219**: 186

Tezel, A., Sens, A., Mitragotri, S. (2003) Description of transdermal transport of hydrophilic solutes during low-frequency sonophoresis based on a modified porous pathway model. *J. Pharm. Sci.* **92**: 381–393

Appendix

Hindered diffusion arises from wall effects when the size of the molecule is comparable with the diameter of the pore. In such a case, the diffusion coefficient of a solute becomes dependent on the ratio of the radius of the solute (a) and the radius of the pore (R_p), $\lambda = a/R_p$. The hindered diffusion coefficient $\overline{D}^M$ is the product of the free diffusion coefficient D_0 and a hindrance coefficient, H_C, which is a function of λ. It was shown by Mavrovouniotis & Brenner (1988) that for small values of λ, the hindrance coefficient can be estimated by:

$$H_C = \frac{1 - \frac{9}{8}\ln\frac{1}{\lambda} - 1.539\lambda}{(1-\lambda)^2} \tag{A1}$$

For $\lambda \to 1$, they showed H_C can be estimated by:

$$H_C = 0.984\left(\frac{1-\lambda}{\lambda}\right)^{\frac{5}{2}} \tag{A2}$$

The hindrance coefficient for intermediate values of λ can be estimated by interpolation between equations A1 and A2.

The Taylor convective dispersion coefficient is defined as (Brenner & Edwards 1993):

$$\overline{D}^C = \frac{R_p^2 \overline{U}^2}{48 D_0} H_D \tag{A3}$$

where $\overline{U}$ is the mean flow velocity, R_P is the pore radius, H_D is a hindrance coefficient and D_0 is the free diffusion coefficient. For ultrasound propagation in a pore, the mean flow velocity is replaced by the root-mean square velocity of the oscillations of fluid molecules in the direction of ultrasound propagation, $\overline{u}$ (Slutsky et al 1980). The root-mean square velocity is related to the amplitude of the acoustic oscillations, u_0, by (Leighton 1994):

$$\overline{u}^2 = \frac{1}{2}u_0^2 \tag{A4}$$

and u_0 is related to the acoustic intensity by (Leighton 1994):

$$u_0^2 = \frac{2I}{\rho c} \tag{A5}$$

hence, $\overline{u}$ is:

$$\overline{u} = \sqrt{\frac{I}{\rho c}} \tag{A6}$$

where I is the ultrasound intensity ($W\,cm^{-2}$), ρ is the density of the medium ($g\,cm^{-3}$), and c is the ultrasound velocity ($cm\,s^{-1}$).

H_D is a coefficient which is a function of λ that accounts for convective dispersive hindrance arising on the pores. For small λ, H_D is given by (Mavrovouniotis & Brenner 1988):

$$H_D = \frac{\lambda^2\left[0.158\ln^2\frac{1}{\lambda} - 0.901\ln\frac{1}{\lambda} + 1.385\right]}{(1-\lambda)^6} \tag{A7}$$

For $\lambda \to 1$, H_D can be estimated by (Mavrovouniotis & Brenner 1988):

$$H_D = 0.0143\left(\frac{1-\lambda}{\lambda}\right)^{\frac{11}{2}} \tag{A8}$$

The Taylor dispersion model given by equation 7 is valid for the viscous flow in pores. Significant viscous effects can be expected during acoustic propagation through pores only when the pore size is sufficiently small such that the acoustic Reynolds number is smaller than some critical value, which is believed to be of order 10 (Slutsky et al 1980). This criterion can be formulated as:

$$Re = \frac{\rho\overline{u}d}{\mu} \leq 10 \tag{A9}$$

where ρ is the density of the medium, $\overline{u}$ is the root-mean square velocity of the molecules in the pore, d is the pore diameter and μ is the dynamic viscosity of the medium. In addition, the Taylor model is only valid for the long-time behaviour of the solute, corresponding to time $t \gg R_p^2/D$. Since it takes a time $t = L/\overline{U}$ for the solute to sample the axial length L, this criterion can be formulated as:

$$\frac{L}{R_P} \gg N_{Pe} \tag{A10}$$

where Pe is the Peclet number:

$$N_{Pe} = \frac{R_P\overline{U}}{D} \tag{A11}$$